Reinforcement of Polyurethane-Based Shape Memory Polymer by Hindered Phenol Compounds and Silica Particles

Mizue Kuriyagawa,[1] Takanobu Kawamura,[1] Shunichi Hayashi,[2] Koh-Hei Nitta[1]

[1]*Division of Material Engineering, Graduate School of Natural Science and Technology, Kanazawa University, Kakuma, Kanazawa, Ishikawa 920-1192, Japan*
[2]*SMP Technologies, Inc., Sendagaya, Shibuyaku, Tokyo 151-0051, Japan*

Received 15 July 2009; accepted 2 January 2010
DOI 10.1002/app.32055
Published online 29 March 2010 in Wiley InterScience (www.interscience.wiley.com).

ABSTRACT: Reinforcement of polyurethane-based shape memory polymer materials was investigated by adding hindered phenol compounds and silica particles. According to dynamic mechanical analysis, these fillers had no effect on the glass transition temperature and the activation energy of soft segments, indicating that the fillers have no ability to influence the molecular mobility of soft segments. It was found from the tensile tests that the yield stress was increased primarily by addition of the hindered phenols rather than the silica particles, whereas Young's modulus was enhanced by the silica particles rather than the hindered phenols. © 2010 Wiley Periodicals, Inc. J Appl Polym Sci 117: 1695–1702, 2010

Key words: mechanical properties; polyurethanes; composites

INTRODUCTION

A polyurethane (PU) is an elastomeric multiblock polymer consisting of chain molecules joined by urethane links, where the urethane hard segments act as crosslinks between amorphous polyether (or polyester) soft segment domains.[1] The soft segments show high mobility and are normally present in coiled form, whereas the hard segments, which are formed from extended isocyanate and are stacked by strong hydrogen bonds, are immobile and rigid. The covalent coupling of the phase-separated hard and soft domains inhibits plastic flow of the chain molecules and leads to elastomeric resiliency under mechanical deformation. The molecular mobility of the soft segments strongly affects the elastomeric properties, and the cohesive force between hard segments plays an important role in the high-tensile strength and mechanical resistance to yielding. In other words, mechanical reinforcement of PU materials can be attained by the improvement of the hard segment interactions, and the glass transition of the soft segments strongly affects the elastomeric elongation and recovery ability.

Shape memory polymers (SMPs) possess the distinctive characteristic that the deformed shape immediately returns to the original shape by heating, enabling unexpected wide applicability such as self-repair and temperature sensing.[2–4] The driving force of shape memory is the elastic strain generated during the deformation. The PU-based SMP are based on a thermoplastic-elastic phase transition, and its reversal at temperatures above and below the glass transition temperature, T_g, of soft segments around frozen hard segments.

Reinforcing of polymers is usually achieved in polymer composites and organic–inorganic hybrids by adding inorganic and/or organic fillers such as particles, fibers, rigid rods, and plates to the polymer matrix. In particular, much attention has recently been paid to nanocomposites by adding nanosized fillers such as organoclay, carbon nanofiber, and silicon carbide. Petrovic et al.[5] showed that silica particles strongly interact with PU matrix, and addition of nanosize silica particles to shape memory PU (SMP) materials enhances strength and elongation at break. In addition, Cho et al.[6] confirmed that the shape memory effect is retained in reinforced SMP/silica hybrids. The X-ray studies on PU/silica composites by Nunes et al.[7] demonstrate that addition of silica to PU causes interactions between the polymer and the hydroxyl groups present on the silica surface. Ohki et al.[8] found that reinforcement of SMP is achieved and the shape memory effect retained by adding glass fibers. Gunes et al.[9] showed that exfoliated organoclay significantly augments shape memory performance, while addition of carbon nanofibers and silicon carbide

Correspondence to: K.-H. Nitta (nitta@t.kanazawa-u.ac.jp).
Contract grant sponsor: SMP Technologies, Inc.

© 2010 Wiley Periodicals, Inc.

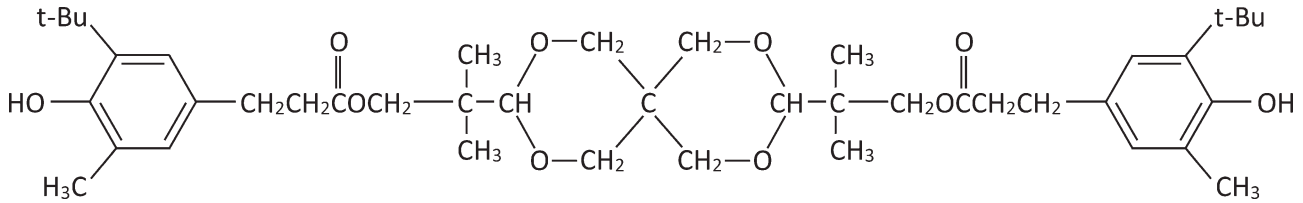

Figure 1 Chemical structure of 3,9-bis[1,1-dimethyl-2{β-(3-*tert*-butyl-4-hydroxy-5-methylphenyl)propionyloxy}ethyl]-2,4,8,10-tetraoxaspiro[5,5]-undecane (AO-80).

diminish it, and addition of carbon black particles destroys the shape memory properties beyond a certain loading.

In general, the hindered phenol compounds have been usually employed as antioxidant additives for various polymers. Wu et al.[10,11] investigated organic–organic hybrids based on rubbery chlorinated polyethylene materials and hindered phenol compounds. They found that addition of hindered phenol compounds to the polymer causes strong hydrogen bonding between hydroxyl groups of the hindered phenol and the α-hydrogen of chlorinated polyethylene, resulting in the emergence of a shape memory effect under a relatively large deformation, which undergoes reorganization and recombination of hydrogen bonds. These results strongly suggest that the additives are capable of operating as reinforcing agents for composites of PU.

In this work, the additive effects of two different types of fillers, spherical inorganic silica particles and organic hindered phenol compounds on reinforcement of SMP were investigated. The objective was to examine the influence of the shape and nature of fillers on the tensile properties of SMP.

EXPERIMENTAL

Materials

A PU-based SMP (DIARY, MM4520: DIAPLEX) was used as the matrix polymer; its weight-average molecular weight (M_w) and molecular weight distribution (M_w/M_n) were 200×10^3 and 2.4, respectively. The SMP is prepared using diphenylmethane-4,4′-diisocyanate (MDI), adipic acid, ethylene glycol, ethylene oxide, polypropylene oxide, 1,4-butanediol, and bisphenol A. It is confirmed that the adipic acid has no ability to form the soft segments and the soft segments are polyether type composed of polypropylene glycol and polyethylene glycol, and the hard segments are aromatic type (MDI). The silica particles and hindered phenol compounds were employed as reinforcements in their composites and hybrids. Spherical SiO_2 (Nano Tek®) with average particle size 26 nm was purchased from Kanto Chemical. The hindered phenol was a commercial antioxidant (ADK STAB AO-80; Asahi Denka Industries), which is 3,9-bis[1,1-dimethyl-2{β-(3-*tert*-butyl-4-hydroxy-5-methylphenyl)propionyloxy}ethyl]-2,4,8,10-tetraoxaspiro[5,5]-undecane (AO-80) (see Fig. 1). Differential scanning calorimetry (DSC) scans showed the glass transition temperature and melting temperature of AO-80 to be 69 and 125°C, respectively.

Sample preparation

SMP pellets were kneaded by mixing rollers at 185°C for 3 min, then a fixed amount from 0 to 10 wt % of AO-80 powder or SiO_2 particles was added to the kneaded SMP, and the mixture kneaded at 185°C for 7 min. The composite sample was then completely melted at 180°C for 5 min between two aluminum plates in a laboratory hot press and pressed at 180°C and 200 kg cm^{-2} pressure for 5 min. On removal from the press, the samples were slowly cooled to room temperature to prepare compression molded films with thickness of about 200 μm for the measurements. The proportion of each filler was changed in the range 0–10 wt %. The characteristics of the samples are given in Table I.

Dynamic mechanical analysis

Dynamic viscoelastic measurements were carried out using a dynamic mechanical analyzer (DVE-V4; Rheology) on rectangular specimens with length 20 mm, width 5 mm, and thickness about 0.2 mm. The measurements were made at constant frequency (10 Hz)

TABLE I
Characteristics of Samples

Sample name	T_g (°C)	ΔH (kJ mol^{-1})	R_g (nm)
SMP	48	530	11
SMP/AO-80(97/3)	48	530	12
SMP/AO-80(95/5)	47	510	12
SMP/AO-80(92/8)	47	510	11
SMP/AO-80(90/10)	48	510	11
SMP/SiO_2(97/3)	50	530	–
SMP/SiO_2(95/5)	49	520	–
SMP/SiO_2(92/8)	49	520	–
SMP/SiO_2(90/10)	50	530	–

T_g, glass transition temperature; ΔH, activation energy of glass transition; R_g, radius of gyration.

with fixed oscillation amplitude (2 μm). The temperature dependences of the tensile storage modulus E', loss modulus E'' and loss tangent tan δ were recorded from 0°C to 100°C at heating rate 2°C min^{-1} under a nitrogen atmosphere. The glass transition temperature of the samples was determined as the temperature corresponding to the sharp relaxation peaks in the E'' curves. The activation energy for the glass transition relaxation process was obtained from the frequency dependence of the dynamic mechanical spectra around T_g.

Tensile tests

Dumbbell shape specimens with gauge length 10 mm, ligament length 4 mm, and overall length 30 mm were used for the tensile tests. The specimens were punched out from compression molded sheets. Uniaxial tensile measurements of the sample specimens were performed with a tensile machine (INSTRON MODEL4466) at 25°C and at fixed crosshead speed (10 mm min^{-1}). The initial distance between clamps was 10 mm. The stress was determined as the tensile load divided by the initial cross-sectional area, and the nominal tensile strain was calculated as the ratio of the increment of the length between clamps to the initial gauge length.

Fourier transform infrared (FTIR) spectroscopy measurements

Infrared spectra were recorded by a Fourier transform infrared (FTIR) spectrometer (ORIEL Instrument MIR8000) at a resolution of 2 cm^{-1} with cumulated number 128 at 21°C. The pellets were completely melted between the naflon sheets at 180°C for 5 min and pressed at 180°C under 750 kg cm^{-2} pressure for 5 min to prepare the thinner films with thickness of 7–9 μm. A Gaussian peak fitting procedure was applied to determine the exact peak position. Data fitting was carried out using the Levenberg–Marquardt algorithm in Wavematrics Igor Pro 4.0 software. The reproducibility of the peak positions was confirmed to be within ±0.05 cm^{-1}. The present computational procedure gave the almost same reproducibility of the peak wavelength as the splain peak fitting procedure for polypropylene and polyethylene.[12,13]

Morphology characterization

The dispersion of the composites was characterized by scanning electron microscopy (SEM) and small angle X-ray scattering (SAXS). SEM images were taken of surfaces formed by fracture in liquid nitrogen then sputter coated with gold using an E-1030 Ionsputter (HITACHI) under low vacuum (60 kg cm^{-2}). The SEM observations were made using an S-4500 (HITACHI) SEM at 15.0 kV. The SAXS measurements were performed in beam line 10C in the Photon Factory, Japan. The samples were irradiated with monochromatized (wavelength, $\lambda = 0.1488$ nm) X-rays radiated from the synchrotron. The scattered X-rays were detected by a one-dimensional position sensitive proportional counter (PSPC).

RESULTS AND DISCUSSION

The SEM images of SMP, SMP/AO-80(92/8), and SMP/SiO_2(92/8) are shown in Figure 2. The magnification of SMP and SMP/AO-80(92/8) micrographs is 10×10^3, and that of SMP/SiO_2(92/8) 30×10^3. Figure 2(c) suggests homogeneous dispersion of silica particles in the matrix: the silica particles can be independently identified, and there are no particle agglomerates. By contrast, there are no objects visible in the SMP/AO-80 hybrids, suggesting that AO-80 was completely dissolved in the matrix. We analyzed the SAXS data to confirm that good miscibility of AO-80 was achieved in the hybrid system. The values of the radius of gyration R_g obtained from Kratky plots (see Fig. 3) were found to be independent of the addition of AO-80 (Table I). This also suggests that AO-80 is completely dissolved in the SMP matrix. The values of R_g were around 11 nm which is the typical order of the domain size of the hard segments of SMP.[14]

The T_g values of SMP/AO-80 hybrids and SMP/SiO_2 composites obtained from dynamic mechanical analysis were very similar to that of pure SMP. Figure 4 shows dynamic mechanical spectra of SMP, SMP/AO-80, and SMP/SiO_2. The glass transition ascribed to the micro-Brownian motion of soft segment chains[4] was clearly observed around 45°C in the spectra. The glass transition temperatures estimated from the E'' peak are listed in Table I. In addition to estimating the activation energy for the relaxation process, we examined the frequency dependence of the E'' peak. A semilogarithmic plot of the frequency against inverse temperature yields the apparent activation energy ΔH. The values of T_g and ΔH (Table I) of hybrids and composites were almost the same for all samples. These results demonstrate that these fillers have no influence on the mobility of the soft segments. The implication is that AO-80 and SiO_2 particles selectively influence the hard segment domains.

Stress–strain curves of SMP, SMP/AO-80(90/10), and SMP/SiO_2(90/10) are exemplified in Figure 5. All of the samples showed a well-defined yield peak and a well-defined neck beyond the yield point. The boundary of the neck propagated under essentially constant flow stress. When the necking boundaries had propagated throughout the entire length of the

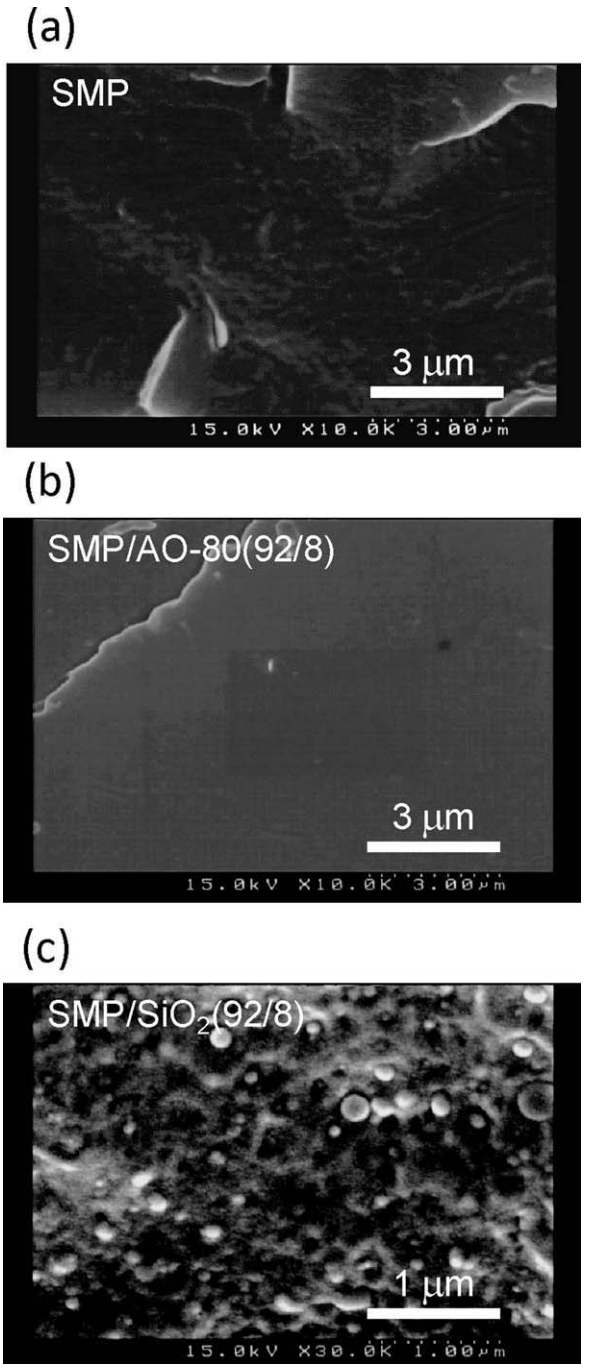

Figure 2 Scanning electron micrographs of drawn samples of (a) SMP, (b) SMP/AO-80 (92/8), and (c) SMP/SiO_2 (92/8).

specimen, the stress increased and the phenomenon of strain hardening appeared, and the specimen fractured. The natural draw ratio was estimated from the elongation at the onset of strain-hardening.

Figure 6 compares the stress–strain curves of SMP measured at −10°C, 25°C, and 45°C at fixed elongation speed 10 mm min^{-1} (strain rate, 1.67% s^{-1}). Embrittlement of SMP occurred below −10°C at that elongation speed, and the material behaved as a typical

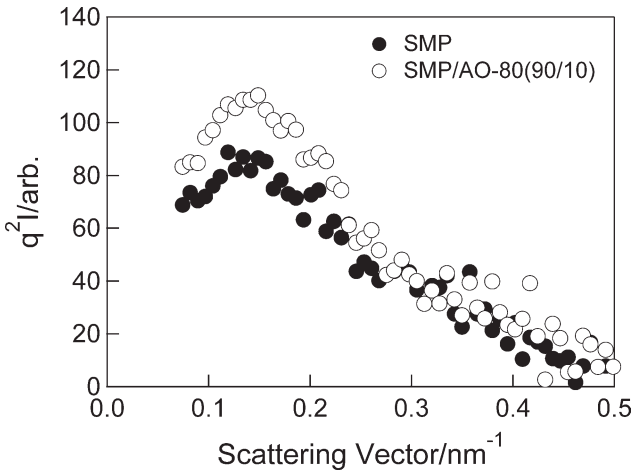

Figure 3 Kratky plot of SAXS data for SMP and SMP/AO-80(90/10).

glassy material, while the SMP behaved like a typical elastomer with no distinct yield point above 45°C because the soft segments were in the rubbery region. The stress–strain curves obtained at room temperature (25°C) closely resemble those of typical semicrystalline polymers such as polyethylene and polypropylene. Thus, the SMP samples acted like leathery materials, suggesting that the soft segments around the hard segment domains are glassy, and the hard segments encapsulated by glassy soft segments act as particulate plastic domains. However, a part of the soft segments or dangling end segments surrounding the particulate domains are considered to be in the rubbery state. The exclusion process of end segments from the particulate domains may result from the spinodal-like process demonstrated by Nitta-Takayanagi.[15] The leathery state is due to

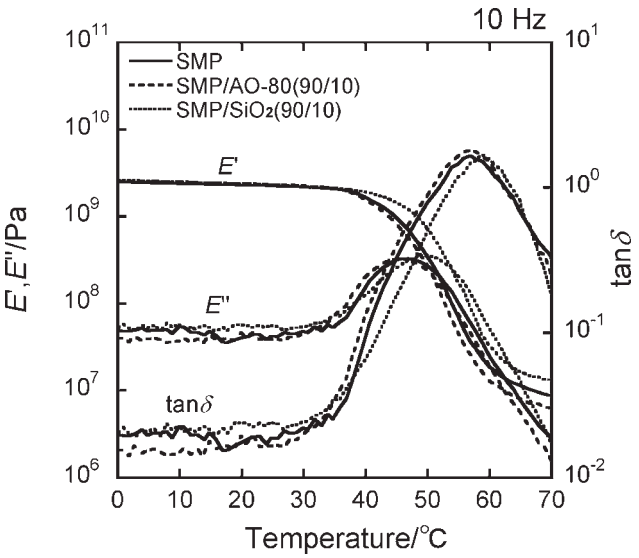

Figure 4 Temperature dependence of storage elastic modulus, loss elastic modulus, and loss tangent of SMP, SMP/AO-80 (90/10), and SMP/SiO_2 (90/10).

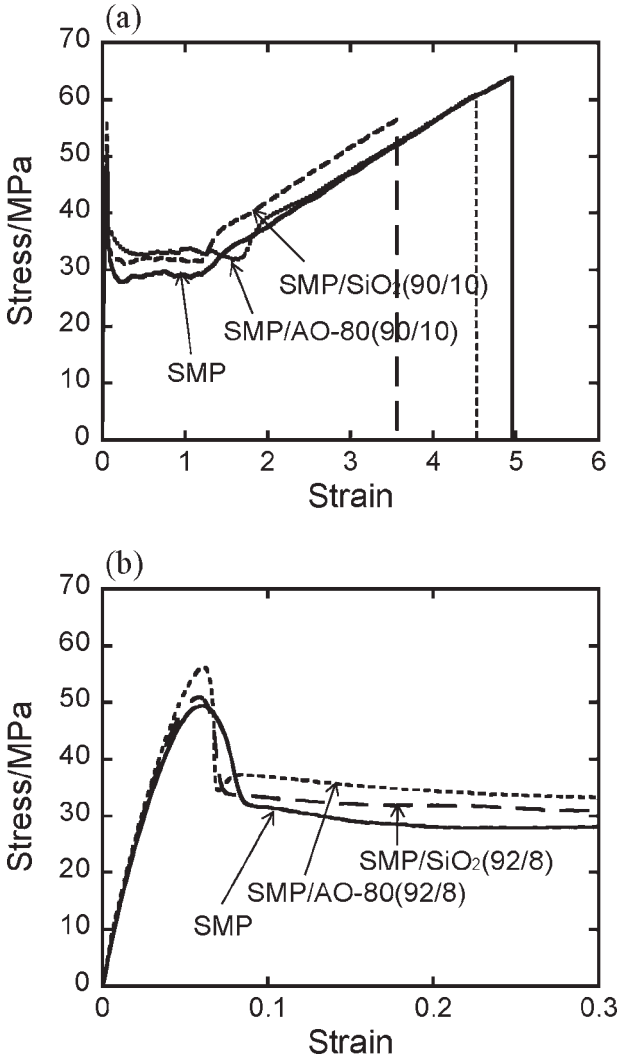

Figure 5 Stress–strain curves of (a) break region and (b) yield region of SMP, SMP/AO-80 (90/10), and SMP/SiO_2 (90/10) measured at 25°C and 10 mm/min.

the fact that the test temperature (25°C) is not very much below T_g (45°C) of the soft segments and is in the plastomer zone.

The Young's modulus values normalized by that of pure SMP are plotted against the content of AO-80 or SiO_2 in Figure 7. Since the test temperature (25°C) is below T_g, Young's modulus of the present samples is predominantly based on the energy elasticity in hard segments and/or the partially glassy state in soft segments, rather than the entropy elasticity caused by micro-Brownian motion. Figure 7 reveals that SiO_2 had a great effect on Young's modulus of SMP, whereas incorporation of AO-80 caused a smaller increase in the modulus. That the size of SiO_2 particles (26 nm) is larger than the domain size of the hard segments (11 nm), and SiO_2 particles have no ability to affect the soft segments, leads us to conclude that the silica particles are located in the particulate plastic domains where the hard segments

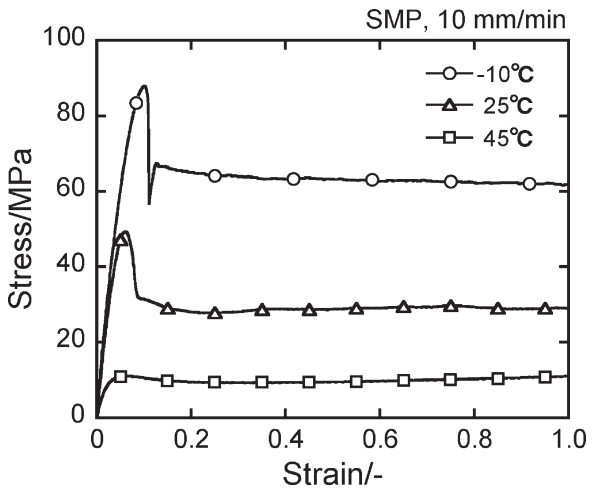

Figure 6 Stress–strain curves of SMP at different temperatures and 10 mm/min.

are surrounded by the leathery soft domains. Thus, the bulkiness of the silica particles offers resistance to the Poisson contraction under tensile deformation, and/or the domain size of hard segments apparently becomes large, resulting in an increase in the modulus. The effect of the addition of silica particles in SMP/SiO_2 thus corresponds to the effect of increase in crystallinity of semicrystalline polymers. The incorporation of AO-80 strengthens the aggregation of hard segments, but AO-80 is considered to be completely dissolved in the particulate plastic domains. Consequently, the domains become stiffer and the domain size is slightly expanded by the dissolution of AO-80. However, the lack of bulkiness of AO-80 fillers is responsible for the insignificant improvement in tensile modulus. Conversely, the addition of AO-80 causes a drastic increase in the yield stress while the magnitude of the increment of the yield stress is lower for SMP/SiO_2, as shown in

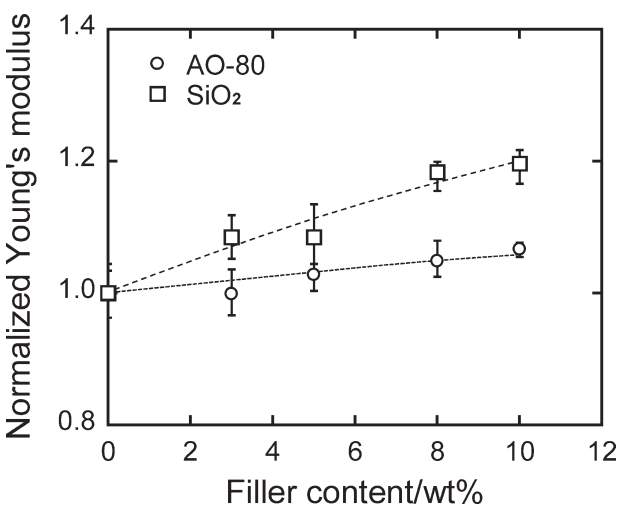

Figure 7 Filler content dependence of Young's modulus normalized by that of pure SMP.

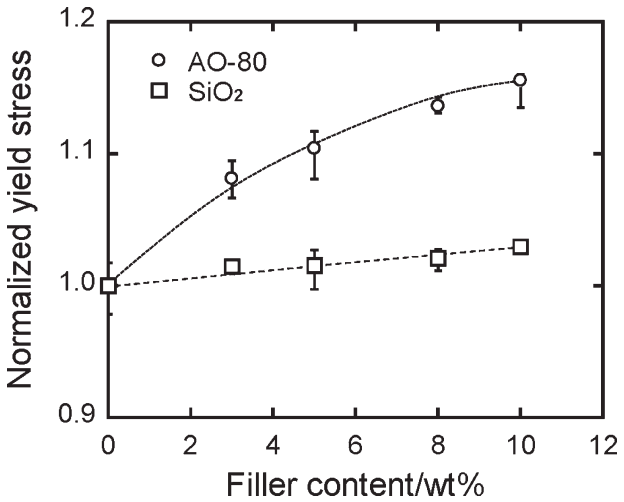

Figure 8 Filler content dependence of yield stress normalized by that of pure SMP.

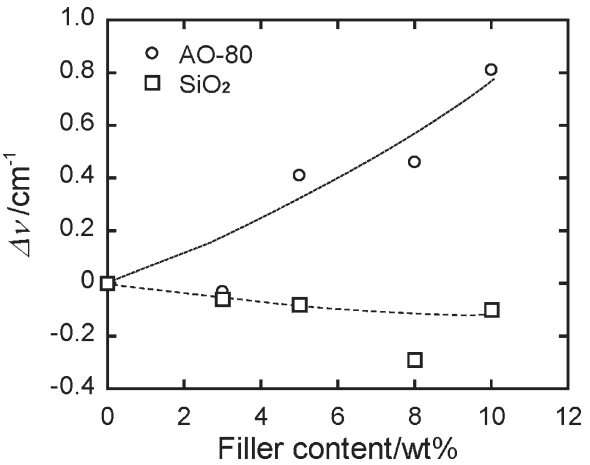

Figure 9 Filler addition-induced wave-number shift plotted against filler content.

Figure 8. This result suggests that the small aspect ratio of the spherical particles is responsible for the insignificant improvement in tensile yield stress.[16] According to *in situ* SAXS measurements under tensile deformation for PU elastomers by Blundell et al.,[17] the hard segments behave as particles embedded in the soft matrix and the mechanical yielding is ascribed to the affine deformation of the particulate hard domains or their affine separation. Although the present materials are not PU elastomers but they behave as PU plastics, the particulate plastic domains, where the hard segments are surrounded by the leathery soft segments, act as a deformation unit under tensile yielding. The yielding process can be considered to be associated with plastic deformation of the domains accompanied by the plastic flow of leathery soft segment domains around the hard segments. The hard domains encapsulated by AO-80 produce high resistance to deformation of the soft domains around the hard segments, so that the incorporation of AO-80 leads to a high-yield stress. The plastic flow process can be analyzed as an Eyring rate process,[18] which will be studied in the near future.

FTIR spectroscopy was measured to investigate the additional effects of fillers on the molecular aggregation states of hard segments and soft segments. The urethane C=O stretching band at 1700 cm^{-1} was apparently splitted into two peaks, which are ascribed to the hydrogen-bond C=O stretching at 1710 cm^{-1} and the free C=O stretching at 1730 cm^{-1}. The peak wave-number shift around 1710 cm^{-1} (H-bonded C=O vibration) was investigated as a function of the content of AO-80 and SiO_2. It was found from Figure 9 that the position of the peak at 1710 cm^{-1} shifts to higher wave-number as the content of AO-80 is increased while the peak position was independent of the addition of SiO_2. The upward shift due to the addition of AO-80 suggests the compression of the C=O bands caused by intense packing of the hard segments. These results correspond to the fact that the addition of AO-80 causes a drastic increase in the yield stress while there is no significant increase of the yield values of SMP/SiO_2. In addition, but not presented here, the peak shift of SMP/AO-80 (90/10) was confirmed to be almost independent of the heat treatment within 18 h at 60°C, suggesting that the interaction between the hard segments and AO-80 is thermally stable.

Proceeding to the elongation beyond the yield point, the cross-section of the sample specimen decreases discontinuously at one point along the gauge length as a neck starts to form. The neck extends along the specimen and the whole specimen is necked at a strain value that is called the natural draw ratio. After the natural draw point, strain

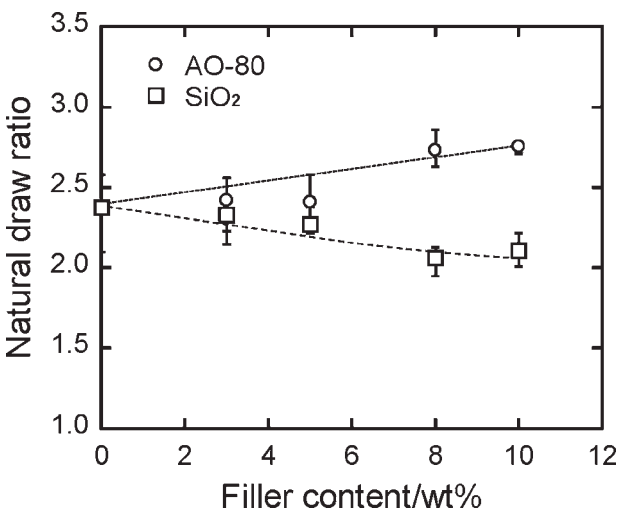

Figure 10 Filler content dependence of natural draw ratio normalized by that of pure SMP.

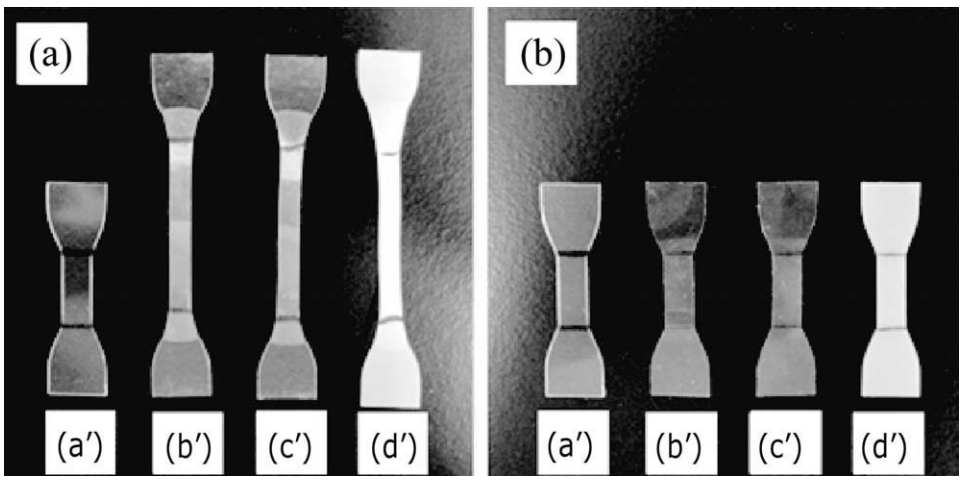

Figure 11 (a) Images of stretched specimens of (a′) original SMP, (b′) stretched SMP, (c′) stretched SMP/AO-80(90/10), and (d′) stretched SMP/SiO_2(90/10). (b) Images of the shape recovered specimens after soaking in hot water.

hardening occurs and the stress rises. The natural draw ratios normalized by that of pure SMP are plotted against SiO_2 and AO-80 contents in Figure 10. It is interesting to note that the natural draw ratio for SMP/SiO_2 decreases with increasing filler content, whereas that for SMP/AO-80 increases with increasing filler content. The decrease in elongation to neck with rigid particles arises from the fact that the actual elongation in the polymer matrix is much greater than the applied elongation of the specimen, and the concentration and localization of elongation between rigid particles cause a reduction in the onset point of the strain hardening, i.e., the natural draw ratio. In the case of SMP/AO-80 systems, the AO-80 dissolves in the hard segment region and has no ability to act as a bulky rigid filler. The addition of AO-80 strengthens the hard segments inside the plastic domains. The tightness of the hard segments acting as physical crosslinks may play an important role in the extensibility in the necked region.[19] In the case of semicrystalline polymers, the natural draw ratio is well known to be higher at higher crystallinity, because the fragmented crystallites behave as physical crosslinks.

Experimental evidence for the chain extension is the thermal shrinkage of drawn polymers on heating above T_g of soft segments. This is a manifestation of the entropic back stress of the stretched chain network, when it is heated to the state of a highly mobile rubber. To confirm the effects of the additions of SiO_2 and AO-80 on the shape memory properties, we observed the shape recovery of deformed specimens. First, deformation up to 3× elongation was applied to the specimen at a fixed crosshead speed of 10 mm min^{-1} at 25°C. The stretched specimens exhibited a necked portion that did not recover promptly to the original length with removal of the load at the test temperature [see Fig. 11(a)]. After immersion for 30 s in hot water at 50°C above T_g, the deformed shape of all samples completely reverted to the original shape of the specimen as shown in Figure 11(b). This result demonstrates that the hard segments are linked with soft segments in a network structure, and the residual entropic extension of soft segments brought about by plastic deformation in the necked region is the origin of the shape recovery effect.

It was found that the reinforcement and improvement of SMP were achieved, keeping the shape memory effect, by incorporating SiO_2 and AO-80. This implies that the hard segments, which act as physical crosslinks, were not damaged beyond the yield point, and the plastic deformation and flow of soft segments surrounding the hard segments are associated with yielding and necking.

CONCLUSION

Different types of reinforcement of PU-based SMP were found to be achieved by adding AO-80 and SiO_2. According to dynamic viscoelastic data, these fillers were confirmed to have no influence on the soft segments of SMP. The tensile tests showed that addition of AO-80 enhances the yield stress, and addition of SiO_2 increases Young's modulus and the stress level in the strain hardening region. These results demonstrate that the nature and shape of fillers independently affects the deformation behavior in the initial strain region, in the yield region and in the strain-hardening region. The bulkiness of spherical inorganic particles is the origin of enhancement of Young's modulus, while the dissolved organic compounds strengthen the interaction between the hard segments, leading to higher resistance to plastic flow. It was confirmed that reinforcement of SMP

was achieved, retaining the shape memory effect, by adding inorganic SiO_2 and organic AO-80.

References

1. Oertel, G. Polyurethane Handbook; Hanser: New York, 1985.
2. Lendlein, A.; Kelch, S. Angew Chem Int Ed 2002, 41, 2034.
3. Takahashi, T.; Hayashi, N.; Hayashi, S. J Appl Polym Sci 1996, 60, 1061.
4. Hayashi, S.; Kondo, S.; Pragna, K.; Ushioda, E. Plast Eng 1995, 51, 29.
5. Petrovic, Z. S.; Javni, I.; Waddon, A.; Banhegyi, G. J Appl Polym Sci 2000, 76, 133.
6. Cho, J. W.; Kim, J. W.; Jung, Y. C.; Goo, N. S. Macromol Rapid Commun 2005, 26, 412.
7. Nunes, R. C. R.; Pereira, R. A.; Fonseca, J. L. C.; Pereira, M. R. Polym Test 2001, 20, 707.
8. Ohki, T.; Ni, Q.-Q.; Ohsako, N.; Iwamoto, M. Compos Part A 2004, 35, 1065.
9. Gunes, I. S.; Cao, F.; Jana, S. C. Polymer 2008, 49, 2223.
10. Wu, C.; Yamagishi, T.-A.; Nakamoto, Y.; Ishida, S.; Nitta, K.-H. J Polym Sci Part B: Polym Phys 2000, 38, 2943.
11. Wu, C.; Yamagishi, T.-A.; Nakamoto, Y.; Ishida, S.; Nitta, K.-H. J Polym Sci Part B: Polym Phys 2000, 38, 2285.
12. Bretzlaff, R. S.; Wool, R. P. Macromoleules 1983, 16, 1907.
13. Wool, R. P.; Bretzlaff, R. S.; Li, B. Y.; Wang, C. H.; Boyd, R. H. J Polym Sci Part B: Polym Phys 1985, 24, 1039.
14. Chang, Y.-J. P. J Polym Sci: Polym Phys Ed 1975, 13, 455.
15. Nitta, K.-H.; Takayanagi, M. J Macromol Sci: Phys B 2003, 42, 107.
16. Nielsen, L. E. Mechanical Properties of Polymers and Composites; Marcel Dekker: New York, 1974; Vol. 2, p 458.
17. Blundell, D. J.; Eeckhaut, G.; Fuller, W.; Mahendrasingam, A.; Martin, C. Polymer 2002, 43, 5197.
18. Halsey, G.; White, H. J.; Erying, H. Text Res J 1945, 15, 295.
19. Niesten, M. C. E. J.; Gayman, R. S. Polymer 2001, 42, 6199.